Search for diastereoisomers of the 3,5-bis(trifluoromethyl)phenyl-dinaphtho propeller crowns: crystal structure and molecular dynamics simulations

William Clegg, Paul J. Cooper, George A. Forsyth and Joyce C. Lockhart
Department of Chemistry, Bedson Building, The University of Newcastle upon Tyne, Newcastle upon Tyne, UK NE1 7RU

The crystal structure of the propeller crown 2-[3,5-bis(trifluoromethyl)phenyl]-4,7,10,13,16,19-hexaoxa-3(1,2),1(2,1)-dinaphthenacyclononadecaphane has been shown to contain the isomer B of the propeller. Molecular dynamics studies of a discrete molecule *in vacuo*, with Coulomb interactions dampened by an effective dielectric constant (relative permittivity), of this and the alternative A isomer help to explain the behaviour of the crown in solution: the propeller section is preorganised while the macrocycle section is mobile on a ps–ns timescale.

Introduction

Crystal structures thus far determined in the propeller crown series[1–5] **1–8** and in the aza-crown series[6] **10–11** have shown the propeller to be present as isomer B (Fig. 1) except for the six-oxygen crown **3** which showed isomer A (Fig. 1).[2] Only in the free ligands of the crown-6 series was any other evidence

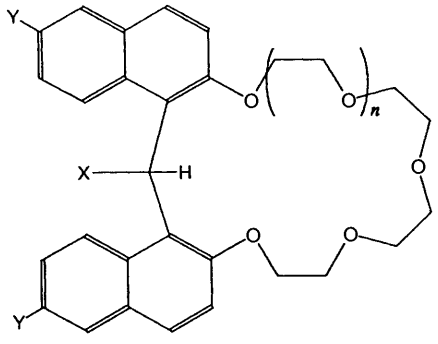

	n	X	Y
1	1	$C_6H_2(OMe)_3$-3,4,5	H
2	2	H	H
3	2	$C_6H_2(OMe)_3$-3,4,5	H
4	1	$C_6H_2(OMe)_3$-3,4,5	H
5	2	$C_6H_2(OMe)_3$-3,4,5	H
6	1	$C_6H_3(Cl)_2$-2,6	H
7	2	C_6H_5	H
8	1	$C_6H_2(OMe)_3$-3,4,5	Bu^t
9	2	$C_6H_3(CF_3)_2$-3,5	H

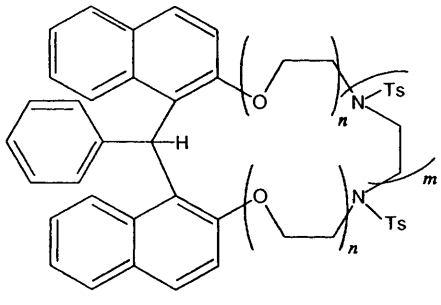

	m	n
10	1	2
11	2	1

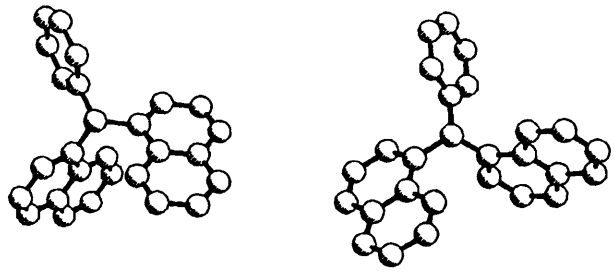

Fig. 1 Propeller sections of isomers A and B

for a second propeller isomer found—in the ^1H NMR spectrum of **3** and in the ^{19}F NMR spectrum of **9** at low temperatures.[3] The $NaBPh_4$ complex of **9** was a single isomer in solution, likewise the KNCS complex of **2**. Signals for two diastereoisomers of the free ligand **9** were seen in the ^{19}F NMR spectrum at 185 K in the ratio 8:3, and two rate processes (which had $\Delta G^{\ddagger}$ 10.8 and 11.6 kcal mol^{-1})† contributed to their averaging, and to the symmetrisation process of the propeller at temperatures up to ambient. The fortuitous isolation of good quality crystals of one isomer of pure ligand **9** from an attempted complexation with a lead salt enabled the determination of its crystal structure. This is presented here together with a molecular dynamics study of the A and B diastereoisomers.

Experimental

The compound 2-[3,5-bis(trifluoromethyl)phenyl]-4,7,10,13,16,19-hexaoxa-3(1,2),1(2,1)-dinaphthenacyclononadecaphane (**9**) was available from previous work[3] and was obtained as crystals from a mixture of lead nitrate and **9** in methanol.

Crystal structure determination‡

Crystal data for 9. $C_{39}H_{36}F_6O_6$, M = 714.7, triclinic, a = 10.737(2), b = 13.633(3), c = 14.052(3) Å, α = 117.952(9), β = 90.485(10), γ = 107.614(10)°, V = 1703.9(6) $Å^3$ (by least-squares refinement on 2θ angles for 32 reflections, λ = 0.710 73 Å, T = 240 K), space group $P\bar{1}$, Z = 2, D_x = 1.393 g cm^{-3}. Colourless crystal, 0.20 × 0.24 × 0.36 mm, μ(Mo-Kα) = 0.114 mm^{-1}, F(000) = 744.

† 1 cal = 4.184 J.

‡ Crystallographic data have been deposited at the Cambridge Crystallographic Data Centre. For details of the deposition scheme, see 'Instructions for Authors (1995)', *J. Chem. Soc., Perkin Trans. 2*, 1995, issue 1.

Table 1 CHARMm parameters for molecular dynamics simulations

	Isomer			
CHARMm term	A	A	B	B
Heating				
IHTFRQ	150	150	150	150
TEMINC	5	5	5	5
NSTEP	6 300	14 100	6300	14 100
FIRSTT	0.0	0.0	0.0	0.0
FINALT	210.0	470.0	210.0	470.0
Equilibration				
IEQFRQ	20	20	20	20
NSTEP	25 000	25 000	25 000	25 000
Simulation				
NSTEP	610 000	610 000	610 000	610 000
Ave. temperature of simulation/K	212	463	206	470

Data collection and processing. Data were collected on a Stoe-Siemens diffractometer in ω/θ scan mode with on-line profile fitting,[7] $2\theta_{max}$ 50°, index ranges h −12 ⟶ 12, k −16 ⟶ 14, l −8 ⟶ 16, no significant variation in intensities of three standard reflections, no absorption corrections, 6079 reflections measured, 6002 unique, R_{int} = 0.114 (on F^2 values).

Structure determination. Solution was by direct methods[8] and difference syntheses, full-matrix least-squares refinement[9] on all measured F^2 values, weighting $w^{-1} = \sigma^2(F^2_o) + (0.0533P)^2 + 1.156P$ where $P = (2F^2_c + F^2_o)/3$. Anisotropic displacement parameters for all non-H atoms, H atoms refined with a riding model in calculated positions, with $U(H) = 1.2U_{eq}(C)$], isotropic extinction parameter $x = 0.0047(9)$ [$F'_c = F_c/(1 + 0.001xF^2_c\lambda^3/\sin 2\theta)^{1/4}$]. Minor disorder components were identified and refined with some restraints for one CF_3 group [occupancy 0.241(4)] and for part of the polyether strand [0.150(4)]. $R' = \{\Sigma[w(F^2_o - F^2_c)^2]/\Sigma[w(F^2_o)^2]\}^{1/2}$ = 0.1398 for all reflections, conventional R = 0.0449 for F values of 4126 reflections having $F^2_o > 2\sigma(F^2_o)$, goodness of fit = 1.053 on all F^2 values for 488 parameters. All features in a final difference synthesis were within ±0.34 eÅ^{-3}.

Molecular dynamics simulations§

The conformational behaviour of isomers A and B was investigated by molecular dynamics (MD) simulations at two temperatures, *ca.* 470 and *ca.* 210 K, both performed *in vacuo*. Energy minimisations of conformations that initiated MD simulations, and all molecular dynamics simulations, were carried out on a Silicon Graphics INDY workstation, using version 22.0 of CHARMm,[10] a commercially available program that is extensively used in the field of small-molecule modelling by this research group (*e.g.* refs. 11 and 12) and other groups (*e.g.* ref. 13). Crystal structure coordinates for isomer B of **9** were used as input for the MD simulation. The isomer A was built from the only crystal structure with that isomer[2] (**3**) and edited, using the Molecular Editor of QUANTA,[14] to replace 3,4,5-$(MeO)_3$ with 3,5-$(CF_3)_2$. These conformations of isomers A and B were used to initiate a 610 ps simulation, at 470 K. Both isomers were also simulated at 210 K, for 610 ps. Conformations that initiated simulations were fully minimised, to remove so-called 'hot-spots', possible unusual or unrealistic geometries, that may result in unusual or unacceptable conformational behaviour during a molecular dynamics simulation. The minimisation procedure was firstly to minimise partially, using 50 steps of the Steepest Descents minimiser, then to fully minimise, using the Adopted-Basis-Newton-Raphson method until convergence was reached (when the first derivative of the energy was < 0.1 kcal mol^{-1}). The molecular dynamics simulations were all 610 ps in duration. The equations of motion were integrated with the Verlet algorithm, with a time-step of 0.001 ps. It was necessary, to achieve the desired simulation temperature (470 or 210 K) to adjust and vary certain CHARMm terms. The relevant terms are listed in Table 1. For isomer A, the heating stage of the dynamics procedure for the simulation at 470 K was to raise the temperature by 5 K (TEMINC) every 0.15 ps (IHTFRQ), from 0 K (FIRSTT) to 470 K (FINALTT), hence NSTEP was set to 14 100. For each molecule a Gaussian distribution of velocities was assigned during heating. During the equilibration stage these velocities were re-scaled every 0.02 ps; the length of equilibration was in each case 25 ps (hence NSTEP was 25 000). Each simulation was continued for 610 ps, with snapshot conformations from the trajectories saved every 1 ps. No bonds were constrained using the SHAKE algorithm.[15] Non-bonded interactions were calculated with a cut-off distance of 15 Å. A shifted cut-off smoothing function was used for van der Waals and electrostatic interactions between 13.5 and 14 Å. A distance-dependent dielectric was used. Atom types and atom charges were assigned using the molecular editor within QUANTA.[14] There were no parameters in the force field of CHARMM 22.0 for the torsion angle defined, using the atom types defined by CHARMM, as X C6R CF3 X, or for the improper angle C6R X X CF3, where X can be any atom, C6R is a carbon atom in a six-membered aromatic ring, and CF3 is a tetrahedral carbon atom specifically attached to three fluorine atoms. These missing terms were approximated by using the published values for the dihedral angle X C6R CT X and the improper angle C6R X X CT, where type CF3 is replaced by type CT, a tetrahedral carbon atom.

Results

The structure of **9** is shown in Fig. 2; the minor disorder components are ignored here. The propeller part of the molecule (Fig. 3) was clearly in the isomer B form. The macrocyclic backbone is illustrated in Fig. 4, with accompanying torsion angles. The torsion angles of the ether strands were: *aaa*, g^+g^+a, ag^-g^+, ag^+g^+, *aaa*. This may be compared with values for **2**, **3** and **7**, the three other propeller crown-6 crystal structures known, in Table 2, which shows the torsion angles in all the known propeller crown crystal structures. Thus, the segment *i*

§ Figs. S1–S13 (movement of torsions) have been deposited under the Supplementary Publications Scheme. For details of the scheme, see 'Instructions for Authors (1995)', *J. Chem. Soc., Perkin Trans. 2*, 1995, issue 1 [Supp. Pub. No. 57092 (14 pp.)].

Table 2 Torsion angles in ether strands observed in propeller crown ethers

Compound	Segment *i*		Segment *ii*		Segment *iii*
1	*aaa*	ag^+a	g^+g^-a	ag^+g^+	
2	g^-g^+a	ag^-a	ag^-g^+	ag^+a	ag^+a
3	g^-g^+a	ag^-a	ag^-g^+	ag^+a	ag^+a
4	g^-aa	ag^+a	g^-g^+a	ag^-a	
5	ag^-a	ag^-a	ag^+a	ag^-a	g^+g^+a
6	ag^+a	g^-g^+a	ag^-g^+	ag^-a	
7	*aaa*	ag^+a	$g^+g^+g^-$	ag^-a	g^-g^+a
8	ag^+a	ag^-a	ag^-a	ag^-a	
9	*aaa*	*aaa*	g^+g^+a	ag^+g^+	ag^-g^+

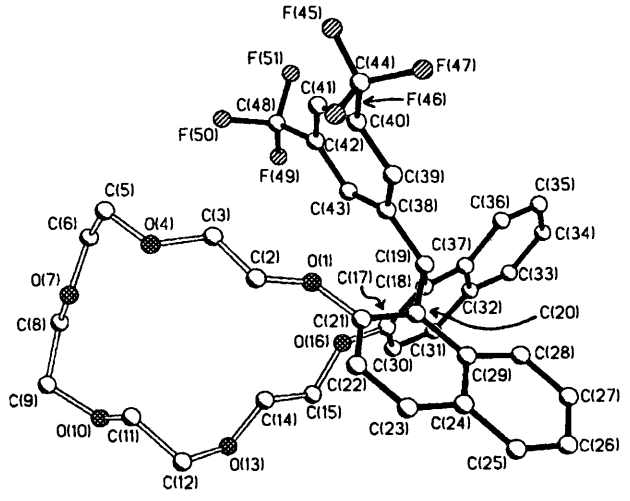

Fig. 2 Structure of **9** showing the labelling of the atoms. Bonds are filled in the propeller substituents, open in the macrocyclic ring. H atoms are omitted.

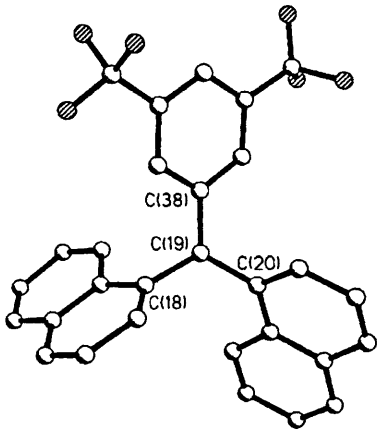

Fig. 3 Propeller section for **9**

torsions in **9** (see Fig. 5 and Table 3 for the definition of segments and torsion angles) are unusual in that both are *anti* (see Fig. 4); only one (naphthyl) O–C–C–O torsion has previously been observed to be *anti*.

Molecular dynamics

Isomer A, 470 K. The propeller of isomer A was essentially static: the torsions C_{ar}–C_{ar}–C–H stayed within a few degrees of the crystal structure value throughout the simulation. Each segment *i* torsion shows a preference for a *gauche* conformation: O(1)–C(2)–C(3)–O(4) spends very little time in an *anti* conformation, but can be seen to flip between *gauche* plus and minus forms very rapidly, between 50 and 300 ps, and between 440 and 500 ps. The overall preference is for a *gauche* minus

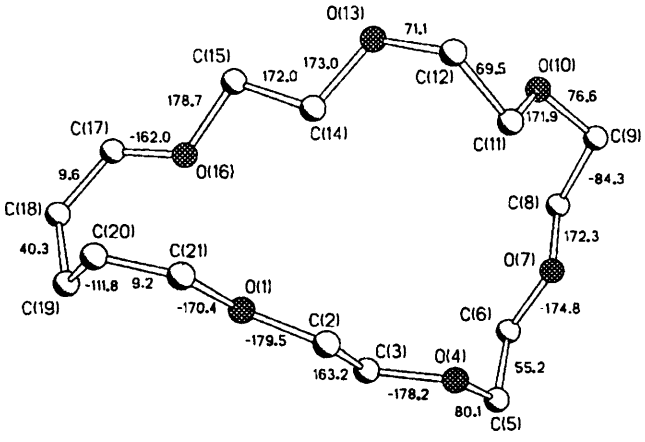

Fig. 4 Torsion angles in the macrocyclic ring of **9**

conformation. There is only one relatively prolonged (*ca.* 50 ps) stay in the *gauche* plus state, between 390 and 440 ps (see Fig. 6); the sister torsion, O(13)–C(14)–C(15)–O(16), shows no prolonged preference for other than *gauche* plus, with brief (5 ps) forays to an *anti* form, or to a *gauche* minus/eclipsed state. The remaining segments were in constant fluctuation: O(4)–C(5)–C(6)–O(7) was in constant motion between *gauche* and *anti* forms, showing no clear preference for a particular value; the other segment *ii* torsion, O(10–C(11)–C(12)–O(13) flipped rapidly (every 5 ps), mainly between *gauche* minus and *anti* forms, with brief excursions to a *gauche* plus state. The segment *iii* torsion behaved in a very similar way to torsion O(4)–C(5)–C(6)–O(7) (see Fig. 7). The average temperature of this simulation was 463 K.

Isomer A, 210 K. At this lower temperature (averaging 212 K for the entire simulation) many of the rapid conformational fluctuations observed at 470 K were slowed or did not occur. No movement from the initial *gauche* plus conformation occurred in the O(13)–C(14)–C(15)–O(16) torsion of segment *i*, but the other segment *i* torsion switched from *gauche* minus to *gauche* plus after 180 ps, for *ca.* 70 ps, and then switched back to the *gauche* minus for the remainder of the simulation. The segment *ii* torsions experienced small fluctuations: O(10–C(11)–C(12)–O(13) underwent a slight change from −80° to −50° after 120 ps, for 80 ps, and again after 460 ps (for 70 ps), and after 550 ps, for the remainder of the simulation except one very brief adjustment to −80°. The other segment *ii* torsion stayed at its initial *gauche* plus state, apart from two very brief flips to *anti*, at 80 and 560 ps; each transition lasted 5 ps. The segment *iii* torsion switched from its initial *anti* conformation to *gauche* plus after 10 ps, staying in this state for 50 ps. This torsion switched back to *anti*, remaining in this conformation until 180 ps had elapsed. During the next *ca.* 270 ps this torsion fluctuated between *gauche* plus and *anti* conformations, before settling in an *anti* state for the rest of the simulation.

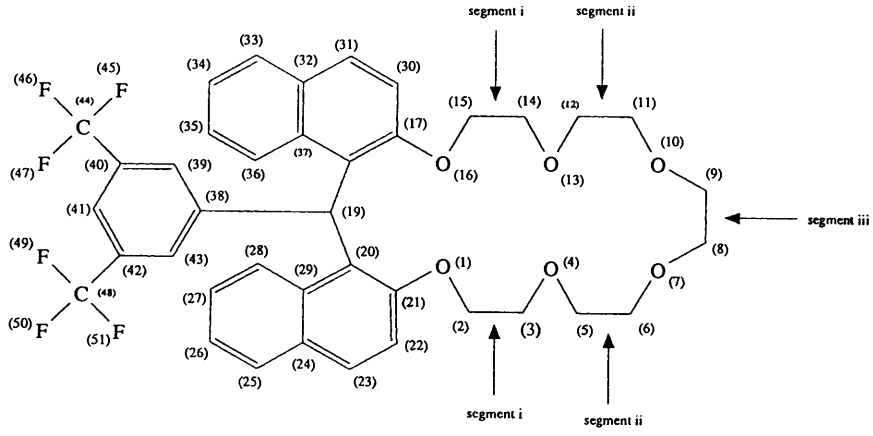

Fig. 5 Line drawing of **9**, showing full atom numbering scheme and definition of segments

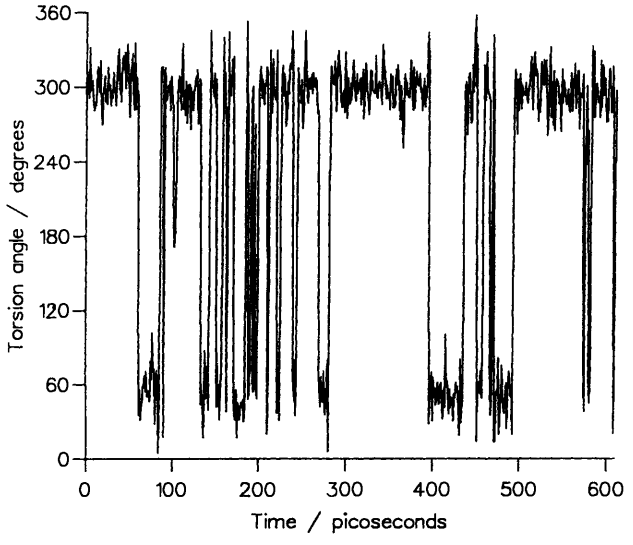

Fig. 6 Movement of torsion O(1)C(2)C(3)O(4) of isomer A of **9** at 470 K over 610 ps

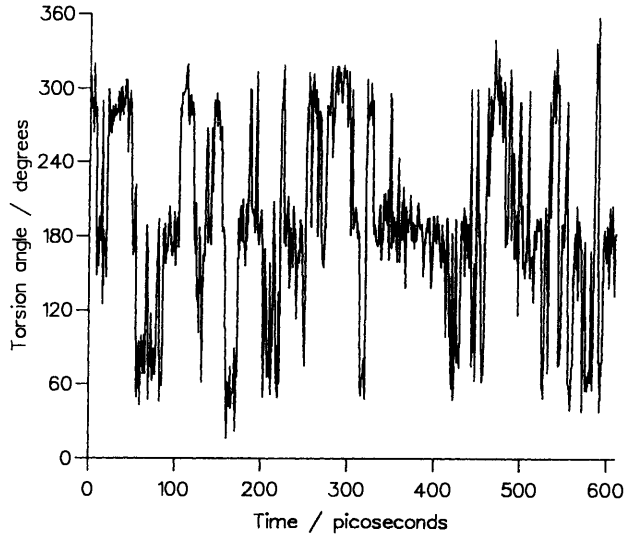

Fig. 7 Movement of torsion O(7)C(8)C(9)O(10) of isomer A of **9** at 470 K over 610 ps

Table 3 Definition of torsion angles in **9**

	Segment	Torsion angle
tor1	*i*	O(1)C(2)C(3)O(4)
tor2	*ii*	O(4)C(5)C(6)O(7)
tor3	*iii*	O(7)C(8)C(9)O(10)
tor4	*ii*	O(10)C(11)C(12)O(13)
tor5	*i*	O(13)C(14)C(15)O(16)
tor6		C(17)C(18)C(19)H(72)
tor7		C(21)C(22)C(19)H(72)
tor8		C(39)C(38)C(19)H(72)

Isomer B, 470 K. The propeller unit does not confer rigidity on the section of the macrocyclic backbone O(1) to O(16): traces of each O–C–C–O torsion show each angle in constant motion between *gauche* and *anti* conformations. The segment *i* torsion O(1)–C(2)–C(3)–O(4) fluctuates at approximately 10 ps intervals between *gauche* and *anti* conformations, with *gauche* plus preferred to *gauche* minus (see Fig. 8). The other segment *i* torsion, O(13)–C(14)–C(15)–O(16), shows a slight preference for *anti* over *gauche*, and no predisposition for either of the *gauche* conformations, but still oscillates between *anti* and *gauche*. Each segment *ii* torsion shows a preference for either *gauche* conformation. Throughout the entire simulation, each

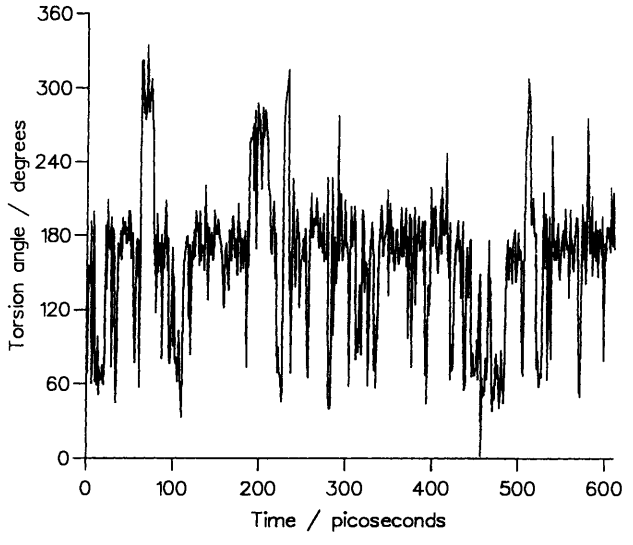

Fig. 8 Movement of torsion O(1)C(2)C(3)O(4) of isomer B of **9** at 470 K over 610 ps

torsion frequently switched from a *gauche* to an *anti* state, or from one *gauche* conformation to the other. The segment *iii*

Table 4 Distribution of torsion angles in isomers A and B from MD simulation at 470 K

Isomer	Segment	Torsion	Percentage		
			anti	*gauche* plus	*gauche* minus
A	*i*	1	10	30	60
	i	5	10	70	20
	ii	2	40	40	20
	ii	4	40	20	40
	iii	3	50	25	25
B	*i*	1	50	40	10
	i	5	60	20	20
	ii	2	20	40	40
	ii	4	33	33	33
	iii	3	10	45	45

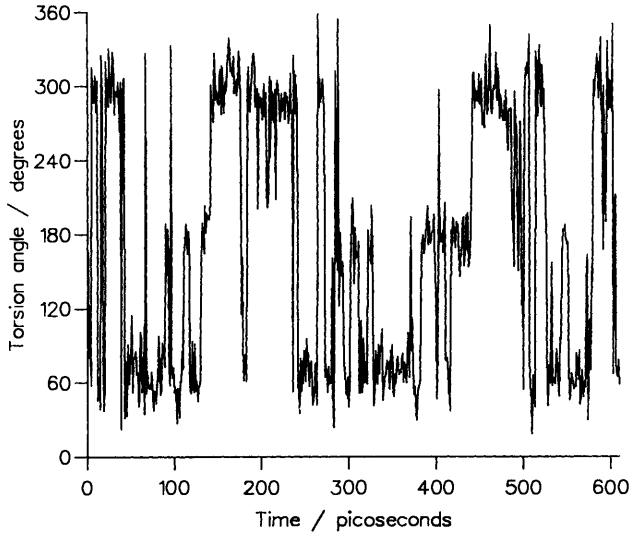

Fig. 9 Movement of torsion O(7)C(8)C(9)O(10) of isomer B of **9** at 470 K over 610 ps

torsion also clearly preferred a *gauche* conformation (see Fig. 9), but was seen to switch from either *gauche* conformation to *anti*, or more usually from *gauche* plus to *gauche* minus (or *vice versa*). The behaviour of the macrocyclic backbone O(1) to O(16) is in marked contrast with the C_{ar}–C_{ar}–C–H torsions of the propeller, which were in effect static throughout the entire simulation. The greatest torsional movement occurred in the C(39)–C(38)–C(19)–H torsion, which swivelled between *ca.* −10° and −60°. The two remaining propeller torsions [C(17)–C(18)–C(19)–H and C(21)–C(20)–C(19)–H] remained at *ca.* 150° for the entire simulation. Traces for torsions C(39)–C(38)–C(19)–H and C(17)–C(18)–C(19)–H are shown in Fig. 10. It was observed, visually using molecular graphics, that the rotation of the phenyl ring is severely restricted due to steric clashes of –C–F and the hydrogens of C(39) and C(43) with the hydrogens of C(3) (of segment *i*) and of C(5) (of segment *ii*).

Isomer B, 210 K. For the entire duration of this simulation, which had an average temperature of 206 K, very little conformational change was observed. Only the segment *iii* torsion, O(7)–C(8)–C(9)–O(10), underwent a prolonged, significant change, from *gauche* minus to *anti*, after 500 ps, which lasted for the remainder of the simulation. The other segment torsion angles remained in their initial states, fluctuating by more than 25° from the crystal structure values, except torsion O(10)–C(11)–C(12)–O(13), which had two brief (5 ps) forays to an *anti* conformer from *gauche* plus. The propeller torsion angles were static, but as was seen with isomer A at a similar temperature, the phenyl 'blade' [C(39)–C(38)–C(19)–H] showed slightly greater movement than the two other 'blades' of the propeller. This almost total lack of torsional movement at the lower temperature displayed by isomer B is probably due to the depth of the potential well in which this particular conformation is found.

Discussion

Certain conformational features of the crystal structure of **9** appeared to be against the trends set for previous propeller crowns. For example, NMR spectroscopy indicated isomers A and B of this molecule to be roughly equal in energy;[3] additionally, the calculated molecular mechanics energy for the crystal structure conformation (isomer B) was 54.76 kcal mol^{-1}, which was similar to the steric energy of the conformation of isomer A built from the crystal structure of **3**, which minimised to 50.44 kcal mol^{-1}. Yet isomer B alone was found in the crystal. Given the NMR evidence and molecular mechanics information relating to the energies of the two isomers, it is likely that crystal packing forces dictate the presence of isomer B.

The observation in the crystal structure of **9** of an *anti* OCCO torsion in both segments *i* was unusual; only three out of the 18 segment *i* torsions previously determined (see Table 2) were *anti*.[1,3,4] However, a distinct preference for a *gauche* placement in segment *i* was found in the simulation of isomer A, with a preference for one segment *i* torsion, O(1)C(2)C(3)O(4), to be fixed and the other [O(13)C(14)-C(15)O(16)] more mobile. This observation of the behaviour of the segment *i* torsions of isomers A and B was previously seen in NMR analyses of coupling constants: for isomer B a slight preference for segment *i* to be *anti* was found, which is consistent with the data available from crystal structures. The proportion of *anti* to *gauche* conformer for each OCCO torsion found for the duration of the simulations is shown in Table 4. The MD data emphasise the extreme mobility of ether segments, indicating that neither isomer could be regarded as having a preorganised macrocycle section. It is also noticeable that although the macrocyclic section of each isomer is very mobile at *ca.* 470 K, there are no patterns of correlated motion for any of the OCCO torsions.

In previous investigations we have used the term 'locked' at timescales too long for the switch of the propeller portion to be observed, and 'mobile' for the propeller viewed under shorter timescales ($\Delta G^{\ddagger}$ being at the lowest, 10–12 kcal mol^{-1} for those propeller crown ethers with unsubstituted phenyl groups). We investigated the mobility of the 'locked' A form at 470 and 210 K, and the locked 'B' form at 470 and at 210 K. Although the propeller switch is a process much too slow to be visualised with molecular dynamics (the ps to ns scale), nevertheless the torsions of the aryl units (propeller blades) are mobile in a more restricted sense. The phenyl group was the most mobile 'blade' in each of the isomers A and B: isomer B in the crystal had the C(39)–C(38)–C(19)–H torsion angle −54° and in the MD simulations this torsion ranged from −80° to 10° centred on the

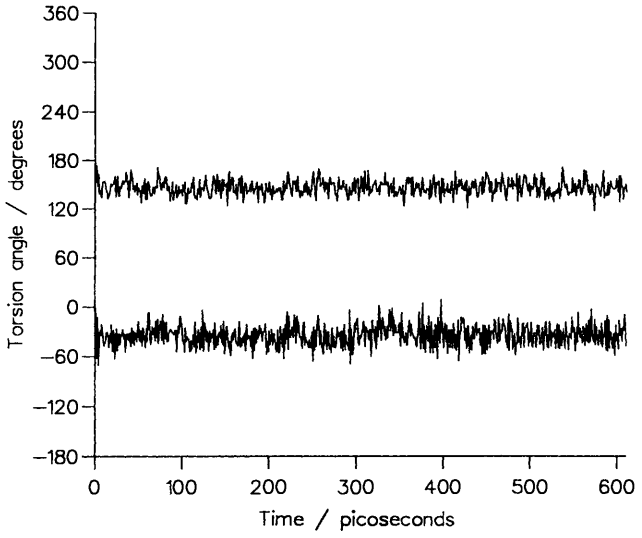

Fig. 10 Movement of torsions C(39)C(38)C(19)H (lower curve) and C(17)C(18)C(19)H (upper curve) of isomer B of **9**, at 470 K over 610 ps

value found in the crystal. The conformers corresponding to these extreme values were each isolated from the trajectory, and fully minimised. They each gave identical propeller conformations, which also superimposed exactly on the propeller of the crystal structure, although the macrocycle sections O(4) to O(13) differed slightly. For isomer A at 470 K, the phenyl torsion was also the most mobile (−120° to −200°), although as expected this movement was much damped at 210 K. The simulations of each isomer have revealed a possible pathway for the propeller flip: in each isomer, the phenyl 'blade' has much the greatest freedom of movement compared with the naphtho 'blades', thus it appears that the phenyl 'blade' may be responsible for initiating the flip.

Conclusions

The movement observed in the molecular dynamics simulations is consistent with the general hypothesis that propeller crowns have fixed, preorganised propeller sections, which restricts movement of at most one adjacent ether segment *i*. The other segments are essentially completely mobile on the ns timescale consistent with NMR solution data; analysis of solution NMR spectra can only give conformational data as statistical averages over many conformations. This is one of the most detailed studies available on the conformational state of fluxional molecules such as propeller crown ethers and has been possible only because of the availability of crystal structures and solution NMR studies which informed the MD studies.

Acknowledgements

The authors are grateful for support from SERC and ICI Specialities (CASE award to P. J. C.; SERC research grant to W. C.) and the Brite-Euram project (contract number BRE2-CT92-0294) of the EU (GAF).

References

1 J. C. Lockhart, M. B. McDonnell and W. Clegg, *J. Chem. Soc., Chem. Commun.*, 1984, 365.
2 W. Clegg, M. B. McDonnell and J. C. Lockhart, *J. Chem. Soc., Perkin Trans. 1*, 1985, 1019.
3 J. C. Lockhart, M. B. McDonnell, W. Clegg and M. N. S. Hill, *J. Chem. Soc., Perkin Trans. 2*, 1987, 639.
4 W. Clegg and J. C. Lockhart, *J. Chem. Soc., Perkin Trans. 2*, 1987, 1621.
5 J. C. Lockhart, M. B. McDonnell, M. N. S. Hill, M. Todd and W. Clegg, *J. Chem. Soc., Dalton Trans.*, 1989, 203.
6 W. Clegg, P. J. Cooper, K. I. Kinnear, D. J. Rushton and J. C. Lockhart, *J. Chem. Soc., Perkin Trans. 2*, 1993, 12.
7 W. Clegg, *Acta Crystallogr., Sect. A*, 1981, **37**, 22.
8 G. M. Sheldrick, SHELXTL/PC Manual, Siemens Analytical X-ray Instruments Inc., Madison, Wi, USA, 1990.
9 G. M. Sheldrick, SHELXTL-93, program for crystal structure refinement, University of Göttingen, 1993.
10 B. R. Brooks, R. E. Bruccoleri, B. D. Olafson, D. J. States, S. Swaminathan and M. Karplus, *J. Comput. Chem.*, 1983, **4**, 1987.
11 G. A. Forsyth and J. C. Lockhart, *Supramolecular Chem.*, 1994, **4**, 17.
12 G. A. Forsyth and J. C. Lockhart, *J. Chem. Soc.*, Dalton Trans., 1994, 2243.
13 J. Beech, P. J. Cragg and M. G. B. Drew, *J. Chem. Soc., Dalton Trans.*, 1994, 719.
14 Quanta 4.0, Molecular Simulations Inc., Waltham, MA, 1994.
15 W. F. van Gunsteren and H. J. C. Berendsen, *Mol. Phys.*, 1977, **34**, 1311.

Paper 5/00606F
Received 1*st February* 1995
Accepted 10*th March* 1995